



Kinetic, isotherm, and thermodynamic investigations of uranium(VI) adsorption on synthesized ion-exchange chelating resin and prediction with an artificial neural network

Hamid Heshmati^{a,*}, Meisam Torab-Mostaedi^b, Hossein Ghanadzadeh Gilani^a, Amir Heydari^c

^aDepartment of Chemical Engineering, University of Guilan, Rasht 41635-3756, Iran, Tel. +98 2182063626; emails: hamid.heshmati25@gmail.com (H. Heshmati), hggilani@guilan.ac.ir (H. Ghanadzadeh Gilani)

^bNuclear Fuel Cycle Research School, Nuclear Science and Technology Research Institute, Tehran, Iran, email: mmostaedi@aeoi.org.ir

^cNuclear Waste Management Company, AEOI, P.O. Box 11365-8486, Tehran, Iran, email: amirheydari110@gmail.com

Received 9 July 2013; Accepted 30 April 2014

ABSTRACT

In this study, an amidoximated chelating ion-exchange resin was prepared using polyacrylonitrile grafted potato starch. The resin characterizations such as specific surface area, pore volume, average pore radius, and Fourier transform infrared spectroscopy of the resin were defined. The effects of pH, contact time, adsorbent dosage, initial concentration of uranium, and temperature on adsorption of uranium ion from aqueous solutions were investigated. The equilibrium adsorption data are fitted Langmuir, Freundlich, Dubinin–Radushkevich (D–R), and Temkin isotherm models and the model parameters are evaluated. The results showed that the D–R model had the best agreement with experimental data. The maximum capacity of adsorption of uranium(VI) onto polyamidoxime resin was found 415.77 mg/g using D–R equation. The kinetic data were well fitted by the pseudo-second-order kinetic model. Thermodynamic parameters including standard enthalpy change (ΔH°), entropy change (ΔS°), and Gibbs free energy (ΔG°) were also determined to specify the type of adsorption reaction using equilibrium constant values at various temperatures. The evaluated ΔH° and ΔG° indicate the endothermic nature of adsorption and the process is spontaneous and favorable. The present study suggests that the prepared adsorbent has promising potential for the removal of uranium(VI) from wastewaters. Furthermore, an artificial neural network (ANN) model was applied to predict adsorption percent of uranium and final pH of solution (pH_f). A good agreement between experimental data and predicted values of applied ANN model was observed.

Keywords: Polyamidoxime; Uranium; Adsorption; Kinetics; Isotherm; Neural network

1. Introduction

Uranium is a toxic radioactive element that is widely distributed over the earth's crust with nuclear

significant. The toxic and dangerous nature of this radionuclide ion is very harmful, even at trace levels, for human physiology and other biological systems and causing various diseases and disorders [1]. Therefore, removal of U(VI) is significant with respect to its industrial importance and toxicity to living beings.

*Corresponding author.

Chemical-precipitation [2], co-precipitation [3], solvent extraction [4], nanofiltration [5], ultrafiltration or polymer-assisted ultrafiltration [6], flotation, ion-exchange [7], adsorption, etc. are the common removing methods which have been developed for preconcentration or separation of uranium from aqueous medium.

The adsorption process was widely used as an effective and convenient method because of its cost-effective treatment and easy operation. Different types of adsorbents such as organic [8,9], inorganic [10–13], biosorbent [14], carbon based material [15,16], etc. have been developed for uranium removal and recovery.

Among the various solid adsorbents, chelating resins are being widely used for the removal of metal ions due to their selectivity and high-adsorption capacity. There are two adopted methods for preparing these chelating materials. One is impregnating the solid substrate with chelating groups and the other one is chemically bonding/grafting the same on the surfaces of solid substrate [17].

The main disadvantage of the first method is leaching of chelating group from solid support which cause to gradual loss of capacity and lifetime [18]. Hence, the preparation of functionalized/grafted resins with suitable functional groups can be developed to overcome this drawback. Selection of appropriate chelating functional group is an important and critical factor to obtain maximum recovery.

There are many researches that explain the synthesis of resins including oxime group by incorporation of a nitrile group to a polymer matrix and converting this group into amidoxime with hydroxylamine in an alkaline medium [19,20]. This macro-reticular chelating resin can be prepared by some different methods such as reacting acrylonitrile–divinylbenzene copolymer with hydroxylamine and synthesis of polyacrylamidoxime resin [21,22]. Another method is incorporation of amidoxime group into cellulose through reaction of cyano ethylcellulose and cyano acrylonitrile with hydroxylamine [23]. The application of divinylbenzene cross-linked polyacrylamidoxime resin has been also investigated on trace metals in natural waters [24].

There are a few publications on the use of PAO resin as a metal adsorbent. In this work, PAO resin has been synthesized for removing of uranium from aqueous solution by batch technique. The effects of various operating parameters such as initial pH of solution, adsorbent dosage, initial ion concentration, contact time, and temperature on the adsorption process are studied. Four different isotherm models are applied to fit the equilibrium data. The adsorption mechanisms of uranium(VI) onto prepared adsorbent

are also evaluated in terms of thermodynamics and kinetics.

Surface complexation modeling can calculate adsorption equilibrium as a function of water chemistry parameter, using mass action and model balance equations [25,26]. There is a big and still growing literature of application of SCM [27–29], and most of them were implemented by chemical equilibrium software programs [26,30]. Although SCM can provide more mechanistic insights to the adsorption equilibrium, ANN models can be practically useful in engineering designs without even using specific chemical equilibrium software programs.

In this work, the experimental data are modeled using ANN model. This model is a system of data processing based on the structure of a biological neural system. This prediction is made by learning of the experimentally generated data or using validated models [31]. The ANN is an artificial intelligence technique imitates the human brain's biological neural network in the problem solving processes. The numerous applications of ANN are conducted to solve environmental problems because of its reliability in capturing the nonlinear relationships existing between variables (multi-input/output) in complex systems [32–34].

In the present work, various experimental parameters such as initial pH, adsorbent dosage, contact time, initial concentration of uranium, and temperature were chosen as inputs variables. The output layer includes two variables such as adsorption percent of uranium and pH_f . On the basis of batch adsorption experiments, a three layer feed forward back propagation ANN model was applied to predict the output parameters.

2. Experimental

2.1. Materials and equipment

Potato starch, methanol, hydroxylamine (50% solution in water), ceric ammonium nitrate, and $UO_2(NO_3)_2 \cdot 6H_2O$ were purchased from Merck. The purities of all chemicals are presented in Table 1. All experiments were carried out using deionized water. Infrared spectrum of PAO was measured with Bruker-Vector22 spectrometer. The macro-pore characterizations of PAO including surface area, average pore volume, and average pore radius were characterized on a Quantocrom surface area apparatus using BET method. The concentration of uranium in the initial solution and supernatant was analyzed by Varian-Liberty 150 AX Turbo as inductively coupled plasma atomic emission spectroscopy.

Table 1
Purity of chemical materials

Component	Supplier	Mass fraction purity
UO ₂ (NO ₃) ₂ ·6H ₂ O	Merck	>0.99
Ceric ammonium nitrate	Merck	>0.99
Potato starch	Merck	>0.99
Methanol	Merck	>0.99
Hydroxylamine	Merck	0.5 (solution in water)
Water		Deionized and bi-distilled

2.2. Synthesis of polyamidoxime chelating ion-exchange resin

2.2.1. Graft copolymerization

About 10 g of potato starch and 400 mL of distilled water were mixed and prepared in a 1,000 mL three-neck flask which was equipped with a condenser, mechanical stirrer, and a thermostat water bath. The prepared slurry was heated for 30 min at 80 °C in presence of an inert gas (N₂ gas). Then, the flask content was cooled to 50 °C and the volume of 8 mL of sulfuric acid (H₂SO₄:H₂O/1:1) was added to the flask. About 40 mL of 0.1 M ceric ammonium nitrate solution was added to the reaction mixture after 5 min and another 10 min later, acrylonitrile monomer (24 mL) was added to the flask. The reaction was completed in 90 min and then the product was cooled by subcooled water. The grafted copolymer was precipitated through washing with methanol solution (methanol:H₂O/4:1) and then dried at 50 °C to a constant weight [35].

2.2.2. Preparation of PAO resin

Treatment of hydroxylamine and nitrile group was done in an alkaline medium (pH 10) in order to prepare the resin containing amidoxime group [24]. This reaction was done using 300 mL of 2.02 M hydroxylamine and 20 g of grafted copolymer which added to a two-neck flask. The flask was equipped with a mechanical stirrer, condenser, and thermostat water bath. The reaction was continued for 2 h at 70 °C. The flask product was filtrated and washed with methanolic solution (methanol:H₂O/4:1). Then, the resin was treated with 0.1 M methanolic solution of hydrochloric acid for 15 min, washed with methanolic solution, and then dried at 50 °C to a constant weight.

2.2.3. Conversion of resin to the H⁺ form

About 11 g of prepared resin was treated with 500 mL of methanolic solution of 0.1 M HCl (methanol:

H₂O/4:1) in a conical flask by batch equilibration and then filtered and washed by methanolic solution.

2.3. Adsorption experiments

Adsorption experiments were performed to obtain the values of optimum pH, optimum PAO dosage, and contact time. The effect of temperature and initial concentration of uranium was also investigated. For each experiment, 100 mL aqueous solution of known concentration of uranium was taken in polyethylene round-bottom flasks containing certain amount of the PAO resin. These flasks were shaken at a constant rate in a temperature controlled rotary shaker. The concentration of uranium was 20 mg/L through all experiments except for those carried out to determine the effect of initial concentration of uranium(VI). The concentration of uranium ion was measured by ICP.

The pH of solution was adjusted in the range of 2–6 using NaOH or HNO₃ aqueous solutions. The effect of adsorbent dosage on UO₂²⁺ removal was studied using 20 mg/L initial uranium concentration with 0.05, 0.1, 0.2, 0.3, 0.4, and 0.5 g/L of PAO resin. Several contact times (5, 10, 20, 30, 45, 60, 75, 90, 120, 150, and 180 min) were applied to obtain the steady state time of adsorption process. Various aqueous solutions of uranyl ion with concentrations of 8.4, 21.1, 49, 73, 94, 150, and 190 mg/L were prepared to study the isotherm models at 25 °C. The calculation of the adsorption uptake (q_e) is given by the mass-balance equation (Eq. (1)):

$$q_e = \frac{V(C_0 - C_e)}{M} \quad (1)$$

where C_0 and C_e are the initial and equilibrium concentration of uranyl ion, respectively. V is the volume of solution (L) and M is the amount of adsorbent (g) used in the adsorption experiment. The percentage of adsorption of metal ions is calculated as follows:

$$\text{Adsorption \%} = \left(\frac{C_0 - C_e}{C_0} \right) \times 100 \quad (2)$$

A blank containing 100 mL of only uranium without any adsorbent was shaken and then passed through the filter to determine any adsorption of uranium ions onto the walls of conical flasks and filter paper. Each experiment was repeated for two times and the mean value was used in all cases.

3. Results and discussion

3.1. Analysis of BET and FT-IR spectrum

Fig. 1 shows the FT-IR spectrum of synthesized chelating PAO resin. The intense and extensive absorption peak at $3,470 \text{ cm}^{-1}$ corresponds to the O–H stretching mode. The bending vibration of N–H bond is observed at peak $1,448 \text{ cm}^{-1}$. The peak observed at $1,108 \text{ cm}^{-1}$ indicates the stretching mode of C–N. The bands at 930 and $1,651 \text{ cm}^{-1}$ are characterized as C=N and N–O stretching mode of oxime groups, respectively [36,37]. The pore structure of PAO resin is given in Table 2 which is analyzed by BET method.

3.2. Effect of pH

The initial pH value of the solution is a significant parameter that must be considered during adsorption studies. Therefore, experiments were carried out in order to investigate the effect of pH on UO_2^{2+} removal by varying the pH from 2.0 to 6.0 (Fig. 2). As shown in Fig. 2, the initial pH of solution is a controlling factor in adsorption of UO_2^{2+} by PAO resin.

The observed lower uptake values of U (VI) at the lowest pH value (pH 2) may be related to the electro-

static repulsion of the protonated active sites of PAO with the positively charged uranyl ions. The $(\text{UO}_2)_2\text{OH}_2^+$ is predominate species in acidic solution up to pH 5 and uranium also exists as a form of $(\text{UO}_2)_3\text{OH}_5^+$ at higher pH values (pH > 5) [38]. As can be seen, the maximum uptake for uranium was found at pH 3. Uranium starts precipitating from solution at pH values higher than 7.0 which makes sorption studies impossible. Therefore, an optimum pH 3.0 is selected for further experiments.

3.3. Effect of adsorbent dosage

The adsorbent dosage is one of the important factors in adsorption process. Fig. 3 shows the effect of PAO dosage on adsorption of UO_2^{2+} ions. As PAO dosage increased from 0.05 to 0.4 g/L the fraction of UO_2^{2+} adsorbed on PAO increased. However, at high-sorbent dosages (more than 0.4 g/L) the available metal ions are insufficient to cover all the exchangeable sites on the PAO resin, resulting in low-metal uptake. So, the optimum PAO dosage was chosen as 0.4 g/L and used for all further experiments.

3.4. Effect of contact time

The sorption of U(VI) on PAO resin was investigated as a function of contact time from 5 to 180 min using initial concentration of 20 mg/L of UO_2^{2+} in aqueous solution. The results of these experiments are illustrated in Fig. 4. This figure shows that the adsorption percentage of UO_2^{2+} increased rapidly within 30 min and attains steady-state condition at about 97% sorption within 120 min. Therefore, the optimum contact time is selected as 120 min for all further experiments.

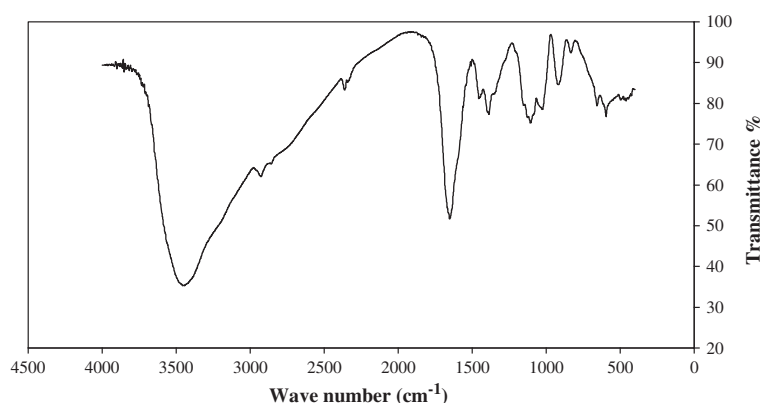


Fig. 1. Infrared spectrum of PAO chelating resin.

Table 2
Porous properties of PAO chelating resin

Resin	Pore volume (mL g ⁻¹) × 10 ³	Surface area (m ² g ⁻¹)	Average pore diameter (nm)
PAO	4.874	6.681	2.918

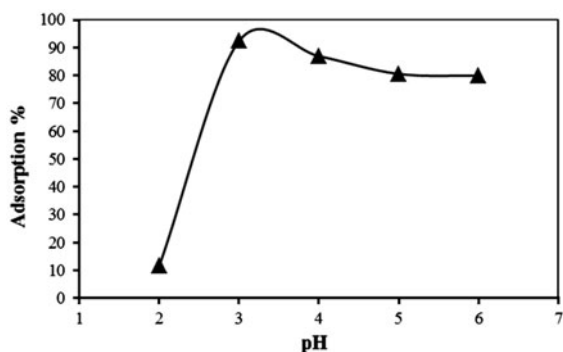


Fig. 2. Effect of pH on uranyl adsorption onto PAO resin for $W = 0.3$ g/L.

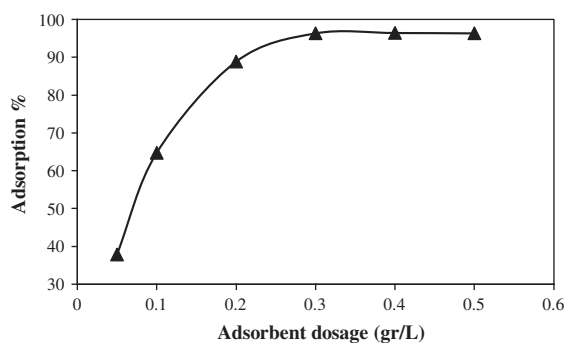


Fig. 3. Effect of PAO dosage on adsorption of uranyl ion at pH 3.

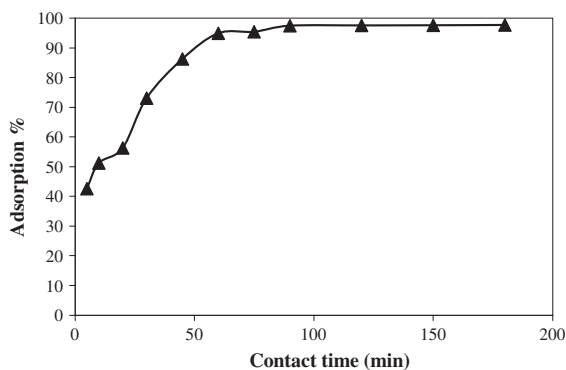


Fig. 4. Effect of contact time on the adsorption of UO_2^{2+} ion by PAO at pH 3 and $W = 0.4$ g/L.

3.5. Adsorption isotherm models

Isotherm models play an important role both in describing the interaction of adsorbate with an adsorbent and in optimizing the use of adsorbent. The Langmuir, Freundlich, Dubinin–Radushkevich (D–R), and Temkin models were selected to analyze the equilibrium data at 25°C. The monolayer sorption on a homogeneous surface without interaction between adsorbed molecules is recommended by Langmuir model [39]. This model includes two constants as q_m and K_L in which q_m is denoted to maximum monolayer sorption capacity of the sorbent (mg/g) and K_L is the Langmuir constant (L/mg) corresponding to the adsorption free energy. The linear and nonlinear equations of Langmuir isotherm model are reported in Table 3. Moreover, a common dimensionless constant called separation factor (R_L) [40] can be expressed in the following equation:

$$R_L = \frac{1}{1 + K_L C_0} \quad (3)$$

The nature of adsorption process can be realized by R_L value to be either unfavorable ($R_L > 1$), linear ($R_L = 1$), favorable ($0 < R_L < 1$), or irreversible ($R_L = 0$). In this study, the R_L value for adsorption of uranyl ion on PAO resin was obtained in the range of 0.067–0.621 which represents a favorable adsorption process.

In order to calculate the q_m and K_L constants, the Langmuir linear equation was applied. These values are reported in Table 4. The evaluated value of q_m illustrates a high ability of PAO resin in adsorption of UO_2^{2+} from aqueous solutions.

The Freundlich isotherm [41] model is an empirical model which is applied for non-ideal and reversible adsorption and also can be used for multilayer adsorption with non-uniform distribution of adsorption affinities and heat over heterogeneous surfaces [42]. This model has an exponential relation with two constant shown in Table 3, where $1/n$ is a numerical value related to sorption intensity varies with the heterogeneity and K_f represents the sorption capacity.

The nature of adsorption process can be determined by analyzing equilibrium data using the D–R

Table 3
List of applied isotherm models

Isotherm	Nonlinear form	Linear form	Plot	Ref.
Langmuir	$q_e = \frac{q_m K_L C_e}{1 + K_L C_e}$	$\frac{C_e}{q_e} = \left(\frac{1}{K_L C_e}\right) + \left(\frac{1}{q_m}\right) C_e$	C_e/q_e vs. C_e	[39]
Freundlich	$q_e = K_f C_e^{1/n}$	$\ln(q_e) = \frac{1}{n} \ln(C_e) + \ln(K_f)$	$\ln(q_e)$ vs. $\ln(C_e)$	[41]
D–R	$q_e = q_{mt} \cdot \exp(-\beta \varepsilon^2)$	$\ln(q_e) = \ln(q_{mt}) - \beta \varepsilon^2$	$-\ln(q_e)$ vs. ε^2	[43]
Temkin	$q_e = \frac{RT}{b_T} \ln(A_T C_e)$	$q_e = \frac{RT}{b_T} \ln(A_T) + \frac{RT}{b_T} \ln(C_e)$	q_e vs. $\ln(C_e)$	[49]

Table 4
Isotherm parameters obtained from Langmuir, Freundlich, D–R, and Temkin models at 25°C

Langmuir		Freundlich		D–R		Temkin	
q_m (mg/g)	K_L (L/mg)	K_f (mg/g)	$1/n$	q_{mt} (mmol/g)	β (mol ² /J ²)	A_T (L ³ /mg)	b_T
416.667	0.076	36.859	0.6087	1.539	1.262×10^{-8}	1.572	0.035

isotherm model [43]. This model describes the adsorption of subcritical vapors onto micropore solids and is generally used to express the adsorption mechanism [44] using a Gaussian energy distribution onto heterogeneous surface [45]. The mathematical expressions of linear and nonlinear forms of the D–R model are presented in Table 3, where q_e is the amount of adsorbed metal ion per unit weight of adsorbent (mol/g), q_{mt} is the maximum capacity of adsorbent (mol/g), β is the activity coefficient (mol²/J²), and ε^2 is the polanyi potential which is depend on temperature and equilibrium concentration of metal ion (C_e) and expressed by the following equation:

$$\varepsilon = RT \ln \left(1 + \frac{1}{C_e} \right) \quad (4)$$

where R is the universal gas constant (8.314 J mol⁻¹ K⁻¹), T is absolute temperature (K), and β value is used to obtain the mean free energy (E , kJ/mol) [46]:

$$E = \frac{1}{\sqrt{2\beta}} \quad (5)$$

The linear form of the D–R model was applied to determine the D–R constants. The results are reported in Table 4. The mechanism of adsorption process can be realized by means of mean free energy. The nature of adsorption process can be physical for the $E < 8$ kJ/mol or chemical for $8 < E < 16$ kJ/mol [47]. Here the mean free energy is 6.294 kJ/mol for adsorption of uranyl ions onto PAO resin and this value shows a physical nature of the adsorption process.

The Temkin isotherm model describes the adsorption of hydrogen onto platinum electrodes in acidic solutions [48]. This isotherm model [49] contains a factor which has an explicit relation between adsorbent and adsorbate interaction. The linear and nonlinear equations of this model are given in Table 3, where b_T is the Temkin isotherm constant and A_T is the Temkin isotherm equilibrium binding constant (L/mg). The linearized form was used to calculate the constants of this isotherm model.

In order to show the agreement of isotherm models with experimental data the R^2 value is reported in this study. Table 5 shows the R^2 values for each isotherm model at 25°C.

According to the reported errors in Table 5, the D–R model has the best agreement with experimental data and can be used to predict the adsorption of uranium(VI) on PAO resin from aqueous solutions at 25°C. Adsorption of uranium(VI) by PAO resin is compared with other adsorbents reported literature in Table 6. The PAO resin should be considered as a suitable adsorbent due to its high ability in adsorption of uranium(VI). Fig. 5

3.6. Adsorption kinetics

Four kinetic models including pseudo-first-order [60], pseudo-second-order [61], Elovich [62], and intraparticle diffusion model [63] were applied to analyze the kinetic of adsorption process. All of linear and nonlinear equations of the above kinetic models are presented in Table 7. In this table, q_t is the amount of metal ion adsorbed (mg/g) at time t (min) and k_1 is adsorption constant (min⁻¹) of pseudo-first-order

Table 5

The R^2 values of four isotherm models for adsorption of uranium(VI) by PAO at 25°C

	Isotherm models			
	Langmuir	Freundlich	D-R	Temkin
R^2	0.926	0.969	0.985	0.910

model. The q_e and k_1 were calculated from the plot of $\ln(q_e - q_t)$ vs. t using the slope and intercept of the plot, respectively. The determined parameters are presented in Table 8.

The k_2 is the constant rate of pseudo-second-order model ($\text{g mg}^{-1} \text{min}^{-1}$). The plot of t/q_t against t can give a linear relation form which k_2 and q_e were calculated from slope and intercept of the plot, respectively.

In Table 7, the α value is the initial rate of adsorption (mg/g min) and β_t is the desorption constant during any experiment for Elovich model (g/mg). Elovich equation was simplified by assuming $\alpha\beta_t t \gg t$ and applying the boundary conditions $q_t=0$ at $t=0$ and $q_t=q_t$ at $t=t$ [55] and the final equation is shown in a linear form in Table 7. The slope and intercept of Elovich model were determined by fitting experimental data through plotting q_t vs. $\ln(t)$.

The equations of intraparticle diffusion model are also given in Table 7, where R_{id} is the percent of U(VI) adsorbed on PAO resin, (t) is the contact time, a describes the adsorption mechanism, and k_{id} is the rate constant of intraparticle diffusion model ($\text{min}^{-1/a}$). The higher values of k_{id} represent an increase in the rate of

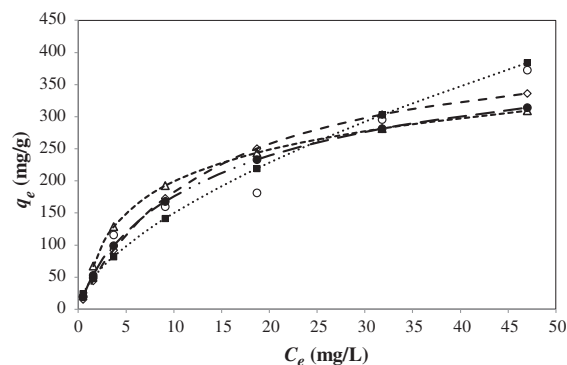


Fig. 5. Comparison of four isotherm models in adsorption of U(VI) by PAO at 25°C; (O) experimental data, (●●●●) Freundlich, (◇◇◇◇) Langmuir, (●●●●) D-R, and (△△△△) Temkin model.

adsorption process and larger a value is related to a better bonding between U(VI) and PAO particles.

All evaluated parameters of four discussed kinetic models and their errors are reported in Table 8. As seen in Table 8, the adsorption kinetics could well be estimated by pseudo-second-order kinetic model. The plot of q_t as a function of time (t) for all discussed kinetic models is illustrated in Fig. 6.

3.7. Thermodynamic parameters

Thermodynamic parameters including enthalpy change (ΔH°), entropy change (ΔS°), and Gibbs free energy (ΔG°) can be determined through following equation:

Table 6

Comparison of adsorption potential of various adsorbents for uranyl ion removal from aqueous solution

Adsorbent	q_{max} (mmol/g)	Ref.
Chitosan/amine resin	1.8	[50]
R1a-mag	1.68	[51]
AXAD-16-3,4-dihydroxybenzoyl methyl phosphonic acid	1.66	[52]
PANSIL at pH 7.5	1.5	[53]
Chitosan/azole resin	1.3	[50]
PANSIL at pH 6	1	[53]
Merrifield chloromethylated	0.96	[54]
Amberlite XAD-16	0.9	[55]
Amberlite XAD-4-Bicene	0.38	[56]
Merrifield polymer-N,N,N,N-tetrahexyl malonamide	0.65	[54]
Goethite	0.114	[57]
Delta MnO ₂	0.564	[58]
Sepiolite (at 30°C)	0.128	[59]
Polyamidoxime chelating resin	1.54	This study

Table 7
Lists of applied kinetic models

Kinetic model	Nonlinear form	Linear form	Plot	Ref.
Pseudo-first-order	$\frac{dq_t}{dt} = k_1(q_e - q_t)$	$\ln(q_e - q_t) = \ln(q_t) - k_1 t$	$\ln(q_e - q_t)$ vs. t	[60]
Pseudo-second-order	$\frac{dq_t}{dt} = k_2(q_e - q_t)^2$	$\frac{t}{q_t} = \frac{1}{k_2 q_e^2} + \left(\frac{1}{q_e}\right) t$	t/q_t vs. t	[61]
Elovich model	$\frac{dq_t}{dt} = \alpha \exp(-\beta_1 q_t)$	$q_t = \frac{1}{\beta_1} \ln(\alpha \beta_1 t) + \frac{1}{\beta_1} \ln(t)$	q_t vs. $\ln(t)$	[62]
Intraparticle diffusion model	$R_{id} = k_{id} t^a$	$\ln(R_{id}) = \ln(k_{id}) + a \ln(t)$	$\ln(R_{id})$ vs. $\ln(t)$	[63]

Table 8
The determined parameters of four kinetic models and their errors for adsorption of U(VI) onto PAO

Pseudo-first-order			Pseudo-second-order		
k_1 (min ⁻¹)	q_e (mg/g)	R^2	k_2 (g/mg min)	q_e (mg/g)	R^2
0.0217	35.705	0.945	4.97×10^{-4}	47.393	0.990
Elovich model			Intraparticle diffusion model		
α (mg/g min)	β_1 (g/mg)	R^2	k_{id} (min ^{-1/a})	a	R^2
0.0288	0.102	0.947	5.288	0.5536	0.957

$$\ln(k_d) = \left(\frac{\Delta S^\circ}{R}\right) - \left(\frac{\Delta H^\circ}{R}\right) \left(\frac{1}{T}\right) \tag{6}$$

where K_d is distribution coefficient and obtain by (Eq. (7)) at various temperatures. The K_d (mL/g) value describes the ratio of uranyl ion in the solid phase over that in the liquid phase and defines the selectivity of the adsorbents for the radioactive element [64]. This coefficient is used for determining thermodynamic parameters by many researchers [65–69].

$$K_d = \frac{V(C_0 - C_e)}{MC_e} \tag{7}$$

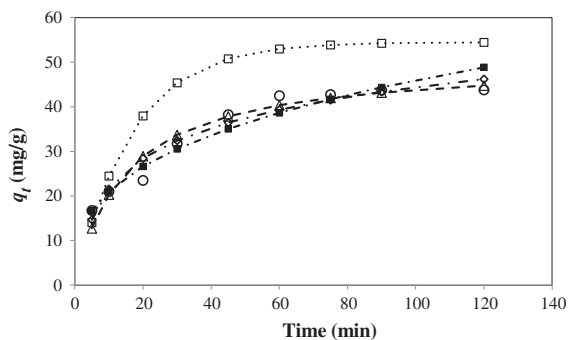


Fig. 6. Comparison of four kinetic models for adsorption of U(VI) by PAO; (O) experimental data, (•□•) pseudo-first-order, (–Δ–) pseudo-second-order, (–◇–) Elovich, and (–■–) intraparticle diffusion model.

The (ΔH°) and (ΔS°) were determined from the slope and intercept of the plotted $\ln(K_d)$ vs. ($1/T$) (Fig. 6). The standard Gibbs free energy change values were also calculated using the following equation:

$$\Delta G^\circ = -RT \ln(K_d) \tag{8}$$

where R is universal gas constant ($8.314 \text{ J mol}^{-1} \text{ K}^{-1}$) and T is absolute temperature. The Gibbs free energy change of the discussed adsorption is also calculated using the equation as below:

$$\Delta G^\circ = \Delta H^\circ - T\Delta S^\circ \tag{9}$$

Table 9 represents the thermodynamic parameters in which negative values of ΔG° show a feasible process and instinctive nature of adsorption of U(VI) onto PAO resin. The ΔH° value also suggests adsorption of U(VI) on PAO chelating resin is endothermic. The positive value of ΔS° indicates that the randomness at the solid–liquid interface during the adsorption process increases (Fig. 7).

Table 9
Thermodynamic parameters for adsorption of U(VI) on PAO at different temperatures

ΔG° (kJ/mol)				ΔH° (kJ/mol)	ΔS° (Jmol ⁻¹ K ⁻¹)
25°C	35°C	45°C	55°C	65.621	243.634
-7.337	-9.428	-10.861	-13.948		

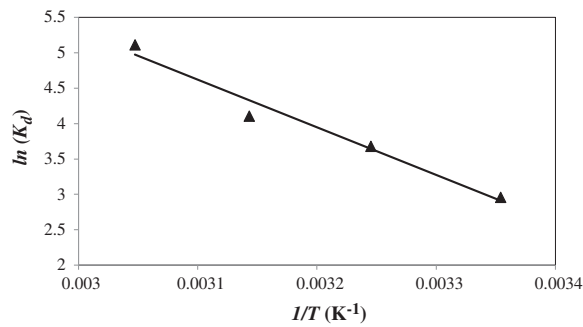


Fig. 7. Variation of $\ln(K_d)$ with $(1/T)$ for adsorption of U(VI) on PAO resin.

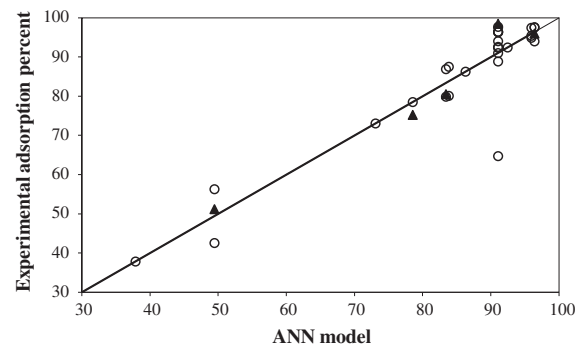


Fig. 8. The training and testing data of applied ANN model for adsorption percent of uranium (ads%); (O) training data and (▲) testing data.

3.8. ANN model

The ANN is widely applied to predict and approximate complex systems which are difficult to model using common modeling techniques such as mathematical modeling. There is no exact available formula to choose a suitable architecture of ANN and training algorithm. The best solution to this limitation is obtained by try and error.

The number of hidden layers, training algorithm, number of neurons in the first and second hidden layers, and transfer functions were obtained by using try and error. The model consisted of two hidden layers with 10 and 11 neurons in the first and second layer, respectively. The best determined transfer/activation functions in both hidden layers were sigmoidal functions and the output layer had a linear transfer function (purelin). The number of training and testing data was 28 and 5 for each output variables, respectively.

The best training algorithm was obtained by Levenberg–Marquardt. Total iteration was set to 2,000 and performance goal was selected as 10^{-5} . The plots of training and testing of experimental data vs. ANN model are presented in Figs. 8 and 9 for the adsorption percent of uranium and pH_f , respectively, which show a good agreement between experimental data

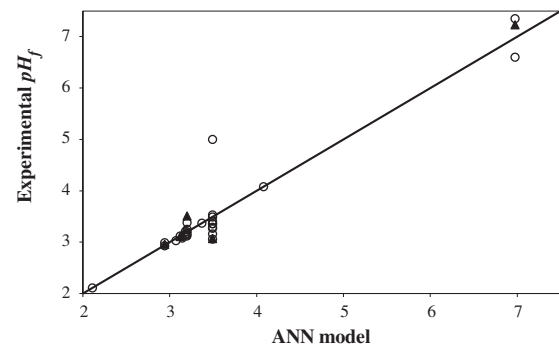


Fig. 9. The training and testing data of applied ANN model for final pH of solution (pH_f); (O) training data and (▲) testing data.

and predicted values of ANN model. The agreement of ANN model was tested by correlation coefficient which expressed as below:

where $M_{cal,i}$ and $M_{exp,i}$ are the calculated and experimental amount of known parameter, respectively. The correlation coefficients (r) of training and testing data of applied ANN model are shown in Table 10.

$$r = \frac{N \sum_{i=1}^N (M_{cal,i} \times M_{exp,i}) - \sum_{i=1}^N (M_{cal,i}) \times \sum_{i=1}^N (M_{exp,i})}{\sqrt{(N \sum_{i=1}^N M_{cal,i}^2 - (\sum_{i=1}^N M_{cal,i})^2) \times (N \sum_{i=1}^N M_{exp,i}^2 - (\sum_{i=1}^N M_{exp,i})^2)}} \quad (10)$$

Table 10
Results of training and testing of applied ANN model

Training			Testing				
NNFHL*	NNSHL**	Transfer functions in both hidden layers	Training algorithm	r (for pH_f)	r (for Ads %)	r (for pH_f)	r (for Ads %)
10	11	Sigmoidal	Levenberg–Marquardt	0.950	0.959	0.989	0.973

*Number of neurons in the first hidden layer.

**Number of neurons in the second hidden layer.

4. Conclusions

In this study, PAO resin was synthesized by means of poly-acrylonitrile (PAN) grafted potato starch and characterized by FT-IR. The average surface area and pore diameter of the resin were found to be $6.681 \text{ m}^2 \text{ g}^{-1}$ and 2.918 nm , respectively. The optimum pH and adsorbent dosage were observed at the amount of 3 and 0.4 g/L , respectively. The D–R isotherm model shows better fit to the sorption data than the other isotherm models. The maximum sorption capacity of PAO for U (VI) was calculated about 415.77 mg/g using D–R model. The kinetics of the process is well described using the pseudo-second-order model. The nature of adsorption process was feasible and endothermic due to positive values of determined ΔG° and ΔH° . Based on the results of the present work, the PAO resin can be used as promising adsorbent for the treatment of wastewaters containing uranyl ions. The determined amounts of correlation coefficients of training and testing data showed a good agreement of obtained values from ANN model with experimental data.

References

- [1] J.D. Van Horn, H. Huang, Uranium(VI) bio-coordination chemistry from biochemical, solution and protein structural data, *Coord. Chem. Rev.* 250 (2006) 765–775.
- [2] A. Mellah, S. Chegrouche, M. Barkat, The precipitation of ammonium uranyl carbonate (AUC): Thermodynamic and kinetic investigations, *Hydrometallurgy* 85 (2007) 163–171.
- [3] J.C. Lozano, F. Fernandez, J.M.G. Gomez, Preparation of alpha-spectrometric sources by co-precipitation with $\text{Fe}(\text{OH})_3$: Application to uranium, *Appl. Radiat. Isot.* 50 (1999) 475–477.
- [4] Y.K. Agrawal, P. Shrivastav, S.K. Menon, Solvent extraction, separation of uranium(VI) with crown ether, *Sep. Purif. Technol.* 20 (2000) 177–183.
- [5] R. Oliver, R.D. Wilken, Removal of dissolved uranium by nanofiltration, *Desalination* 122 (1999) 147–150.
- [6] A.P. Kryvoruchko, L.Y. Yurlova, I.D. Atamanenko, B.Y. Kornilovich, Ultrafiltration removal of U(VI) from contaminated water, *Desalination* 162 (2004) 229–236.
- [7] T. Prasada Rao, P. Metilda, J.M. Gladis, Preconcentration technique for uranium(VI) and uranium(IV) prior to analytical determination, *Talanta* 68 (2006) 1047–1064.
- [8] M.K. Sureshkumar, D. Das, M.B. Mallia, P.C. Gupta, Adsorption of uranium from aqueous solution using chitosan-tripolyphosphate (CTPP) beads, *J. Hazard. Mater.* 184 (2010) 65–72.
- [9] X. Sun, X. Huang, X.P. Liao, Adsorptive recovery of UO_2^{2+} from aqueous solutions using collagen–tannin resin, *J. Hazard. Mater.* 179 (2010) 295–302.
- [10] F.L. Fan, Z. Qin, J. Bai, W.D. Rong, F.Y. Fan, W. Tian, X.L. Wu, Y. Wang, L. Zhao, Rapid removal of uranium from aqueous solutions using magnetic $\text{Fe}_3\text{O}_4@-\text{SiO}_2$ composite particles, *J. Environ. Radio.* 106 (2012) 40–46.
- [11] A. Kilislioglu, B. Bilgin, Adsorption of uranium on halloysite, *Radiochim. Acta* 90 (2002) 155–160.
- [12] Z.J. Guo, H.Y. Su, W.S. Wu, Sorption and desorption of uranium(VI) on silica: experimental and modeling studies, *Radiochim. Acta* 97 (2009) 133–140.
- [13] S. Li, H. Bai, J. Wang, X. Jing, Q. Liu, M. Zhang, R. Chen, L. Liu, C. Jiao, In situ grown of nano-hydroxyapatite on magnetic CaAl-layered double hydroxides and its application in uranium removal, *Chem. Eng. J.* 193–194 (2012) 372–380.
- [14] M. Ghasemi, A.R. Keshkar, R. Dabbagh, S.J. Jaber Safdari, Biosorption of uranium(VI) from aqueous solutions by Ca-pretreated *Cystoseira indica* alga: Breakthrough curves studies and modeling, *J. Hazard. Mater.* 189 (2011) 141–149.
- [15] A.M. Starvin, T.P. Rao, Solid phase extractive preconcentration of uranium(VI) onto diarylazobisphenol modified activated carbon, *Talanta* 63 (2004) 225–232.
- [16] A.K. Singha Deb, P. Ilaiyaraja, D. Ponraju, B. Venkatraman, Diglycolamide functionalized multi-walled carbon nanotubes for removal of uranium from aqueous solution by adsorption, *J. Radioanal. Nucl. Chem.* 291 (2012) 877–883.
- [17] B. Gao, Y. Gao, Y. Li, Preparation and chelation adsorption property of composite chelating material poly(amidoxime)/ SiO_2 towards heavy metal ions, *Chem. Eng. J.* 158 (2010) 542–549.
- [18] M.S. Hosseini, A.H. Hosseini-Bandegharai, Comparison of sorption behavior of Th(IV) and U(VI) on modified impregnated resin containing quinizarin with that conventional prepared impregnated resin, *J. Hazard. Mater.* 190 (2011) 755–765.

- [19] N. Kabay, H. Egawa, Preparation and characterization of amidoxime resins based on poly(acrylonitrile-co-vinylidene chloride-co-divinylbenzene), *J. Appl. Polym. Sci.* 51 (1994) 381–387.
- [20] N. Kabay, T. Hayashi, A. Jyo, H. Egawa, Amidoxime resins based on poly(acrylonitrile-co-vinylidene chloride-co-divinylbenzene) and their behavior in uptake of uranium from sea water, *J. Appl. Polym. Sci.* 54 (1994) 333–338.
- [21] H. Egawa, N. Kabay, T. Shuto, A. Jyo, Recovery of uranium from seawater. XII. Preparation and characterization of lightly crosslinked highly porous chelating resins containing amidoxime groups, *J. Appl. Polym. Sci.* 46 (1992) 129–142.
- [22] Y. Kobuke, H. Tanaka, H. Ogoshi, Imidedioxime as a significant component in so-called amidoxime resin for uranyl adsorption from seawater, *Polym. J.* 22 (1990) 179–182.
- [23] C.A. Fetscher, US Patent 3088798, 1963.
- [24] R. Lei, X. Jie, X. Jun, Z. Ruiyun, Structure and properties of polyvinyl alcohol amidoxime chelate fiber, *J. Appl. Polym. Sci.* 53 (1994) 325–329.
- [25] J.A. Davis, D.B. Kent, Surface complexation modeling in aqueous geochemistry, *Rev. Mineral. Geochem.* 23 (1) (1990) 177–260.
- [26] Z. Wang, D.E. Giammar, Mass action expressions for bidentate adsorption in surface complexation modeling: Theory and practice, *Environ. Sci. Technol.* 47(9) (2013) 3982–3996.
- [27] M.O. Barnett, P.M. Jardine, S.C. Brooks, U(VI) adsorption to heterogeneous subsurface media: Application of a surface complexation model, *Environ. Sci. Technol.* 36(5) (2002) 937–942.
- [28] G.Z. Nie, B.C. Pan, S.J. Zhang, B.J. Pan, Surface chemistry of nanosized hydrated ferric oxide encapsulated inside porous polymer: Modeling and experimental studies, *J. Phys. Chem. C* 117(12) (2013) 6201–6209.
- [29] Y. Wang, J. Wu, Z. Wang, A. Terenyi, D.E. Giammar, Kinetics of lead(IV) oxide (PbO₂) reductive dissolution: Role of lead(II) adsorption and surface speciation, *J. Colloid Interface Sci.* 389(1) (2013a) 236–243.
- [30] C. Koretsky, The significance of surface complexation reactions in hydrologic systems: A geochemist's perspective, *J. Hydrol.* 230(34) (2000) 127–171.
- [31] M.R. Fagundes-Klen, P. Ferri, T.D. Martins, C.R.G. Tavares, E.A. Silva, Equilibrium study of the binary mixture of cadmium–zinc ions biosorption by the *Sargassum filipendula* species using adsorption isotherms models and neural network, *Biochem. Eng. J.* 34 (2007) 136–146.
- [32] S. Aber, A.R. Amani-Ghadim, V. Mirzajani, Removal of Cr(VI) from polluted solutions by electrocoagulation: Modeling of experimental results using artificial neural network, *J. Hazard. Mater.* 171 (2009) 484–490.
- [33] D. Salari, N. Daneshvar, F. Aghazadeh, A.R. Khataee, Application of artificial neural networks for modeling of the treatment of wastewater contaminated with methyl tert-butyl ether (MTBE) by UV/H₂O₂ process, *J. Hazard. Mater.* 125 (2005) 205–210.
- [34] K. Yetilmezsoy, S. Demirel, Artificial neural network (ANN) approach for modeling of Pb(II) adsorption from aqueous solution by antep pistachio (*Pistacia Vera L.*) shells, *J. Hazard. Mater.* 153 (2008) 1288–1300.
- [35] M. Liu, R. Cheng, J. Wu, C. Ma, Graft copolymerization of methyl acrylate onto potato starch initiated by ceric ammonium nitrate, *J. Polym. Sci., Part A* 31 (1993) 1381–1386.
- [36] T. Hirotsu, S. Katoh, K. Sugasaka, N. Takai, M. Seno, T. Itagaki, Adsorption of uranium on cross-linked amidoxime polymer from seawater, *Ind. Eng. Chem. Res.* 26 (1987) 1970–1977.
- [37] T. Hirotsu, S. Katoh, K. Sugasaka, N. Takai, M. Seno, T. Itagaki, Effect of water content of hydrophilic amidoxime polymer on adsorption rate of uranium from seawater, *J. Appl. Polym. Sci.* 36 (1988) 1741–1752.
- [38] T. Prasada Rao, P. Metilda, J. Mary Gladis, Preconcentration techniques for uranium(VI) and thorium(IV) prior to analytical determination: An overview, *Talanta* 68 (2006) 1047–1064.
- [39] I. Langmuir, The constitution and fundamental properties of solids and liquids. Part I. Solids, *J. Am. Chem. Soc.* 38 (1916) 2221–2295.
- [40] T.W. Weber, R.K. Chakravorty, Pore and solid diffusion models for fixed-bed adsorbers, *AIChE J.* 20 (1974) 228–238.
- [41] H.M.F. Freundlich, Over the adsorption in solution, *J. Phys. Chem.* 57 (1906) 385–471.
- [42] A.W. Adamson, A.P. Gast, *Physical Chemistry of Surfaces*, 6th ed., Wiley-Interscience, New York, NY, 1997.
- [43] M.M. Dubinin, L.V. Radushkevich, The equation of the characteristic curve of the activated charcoal, *Proc. Acad. Sci. USSR Phys. Chem. Sect.* 55 (1947) 331–337.
- [44] A. Günay, E. Arslankaya, I. Tosun, Lead removal from aqueous solution by natural and pretreated clinoptilolite: Adsorption equilibrium and kinetics, *J. Hazard. Mater.* 146 (2007) 362–371.
- [45] A. Dąbrowski, Adsorption—From theory to practice, *Adv. Colloid Interface Sci.* 93 (2001) 135–224.
- [46] F. Helfferich, *Ion Exchange*, McGraw Hill, New York, NY, 1962.
- [47] A. Sari, M. Tuzen, Removal of mercury(II) from aqueous solution using moss (*Drepanocladus revolvens*) biomass: Equilibrium, thermodynamic and kinetic studies, *J. Hazard. Mater.* 171 (2009) 500–507.
- [48] K.Y. Foo, B.H. Hameed, Insights into the modeling of adsorption isotherm systems, *Chem. Eng. J.* 156 (2010) 2–10.
- [49] M.I. Temkin, V. Pyzhev, Kinetics of ammonia synthesis on promoted iron catalyst, *Acta Phys. Chem.* 12 (1940) 327–356.
- [50] A.A. Atia, Studies on the interaction of Mercury(II) and Uranyl(II) with modified chitosan resins, *Hydrometallurgy* 80 (2005) 13–22.
- [51] A.M. Donia, A.A. Atia, E.M.M. Moussa, A.M. El-Sherif, M.O. Abd El-Magied, Removal of uranium(VI) from aqueous solutions using glycidyl methacrylate chelating resins, *Hydrometallurgy* 95 (2009) 183–189.
- [52] M.A. Maheswari, M.S. Subramanian, AXAD-16-3, 4-dihydroxy benzoyl methyl phosphonic acid: A selective preconcentrator for U and Th from acidic waste streams and environmental samples, *React. Funct. Polym.* 62 (2005) 105–114.
- [53] C.S. Barton, D.I. Stewart, K. Morris, D.E. Bryant, Performance of three resin-based materials for treating uranium-contaminated groundwater within a PRB, *J. Hazard. Mater.* 116 (2004) 191–204.

- [54] C.S.K. Raju, M.S. Subramanian, Selective preconcentration of U(VI) and Th(IV) in trace and macroscopic levels using malonamide grafted polymer from acidic matrices, *Microchim. Acta* 150 (2005) 297–304.
- [55] M. Merdivan, M.Z. Düz, C. Hamamci, Sorption behaviour of uranium(VI) with N,N-dibutyl-N'-benzoylthiourea impregnated in Amberlite XAD-16, *Talanta* 55 (2001) 639–645.
- [56] P. Metilda, K. Sanghamitra, J.M. Gladis, G.R.K. Naidu, T. Prasada, Rao, Amberlite XAD-4 functionalized with succinic acid for the solid phase extractive preconcentration and separation of uranium(VI), *Talanta* 65 (2005) 192–200.
- [57] D.E. Giammar, J.G. Hering, Time scales for sorption–desorption and surface precipitation of uranyl on goethite, *Environ. Sci. Technol.* 35 (2001) 3332–3337.
- [58] Z. Wang, S.W. Lee, J.G. Catalano, J.S. Lezama-Pacheco, J.R. Bargar, B.M. Tebo, D.E. Giammar, Adsorption of uranium(VI) to manganese oxides: X-ray absorption spectroscopy and surface complexation modeling, *Environ. Sci. Technol.* 47(2) (2013b) 850–858.
- [59] R. Donat, The removal of uranium(VI) from aqueous solutions onto natural sepiolite, *J. Chem. Thermodynamics* 41 (2009) 829–835.
- [60] S. Lagergren, About the theory of so-called adsorption of soluble substances, *K. Sven. Vetenskapsakademien. Handl.* 24 (1898) 1–39.
- [61] Y.S. Ho, G. McKay, Pseudo-second order model for sorption processes, *Process Biochem.* 34 (1999) 451–465.
- [62] S.H. Chien, W.R. Clayton, Application of Elovich equation to the kinetics of phosphate release and sorption in soils¹, *Soil Sci. Soc. Am. J.* 44 (1980) 265–268.
- [63] S.K. Srivastava, R. Tyagi, N. Pant, Adsorption of heavy metal ions on carbonaceous material developed from the waste slurry generated in local fertilizer plants, *Water Res.* 23 (1989) 1161–1165.
- [64] L.L. Ames, Kinetics of cesium reactions with some inorganic cation exchange materials, *Am. Miner.* 47 (1962) 1067–1078.
- [65] D. Baybaş, U. Ulusoy, The use of polyacrylamide-aluminosilicate composites for thorium adsorption, *App. Clay. Sci.* 51 (2011) 138–146.
- [66] Z. Talip, M. Eral, Ü. Hiçsönmez, Adsorption of thorium from aqueous solutions by perlite, *J. Environ. Rad.* 100 (2009) 139–143.
- [67] R. Akkaya, U. Ulusoy, Tl-208, Pb-212, Bi-212, Ra-226 and Ac-228 adsorption onto polyhydroxyethylmethacrylate–bentonite composite, *Nucl. Instrum. Methods Phys. Res., Sect. A* 664 (2012) 98–102.
- [68] S.M. Yu, C.L. Chen, P.P. Chang, T.T. Wang, S.S. Lu, X.K. Wang, Adsorption of Th(IV) onto Al-pillared rectorite: Effect of pH, ionic strength, temperature, soil humic acid and fulvic acid, *Appl. Clay Sci.* 38 (2008) 219–226.
- [69] A. Kaygun, S. Akyil, Study of the behaviour of thorium adsorption on PAN/Zeolite composite adsorbent, *J. Hazard. Mater.* 147 (2007) 357–362.